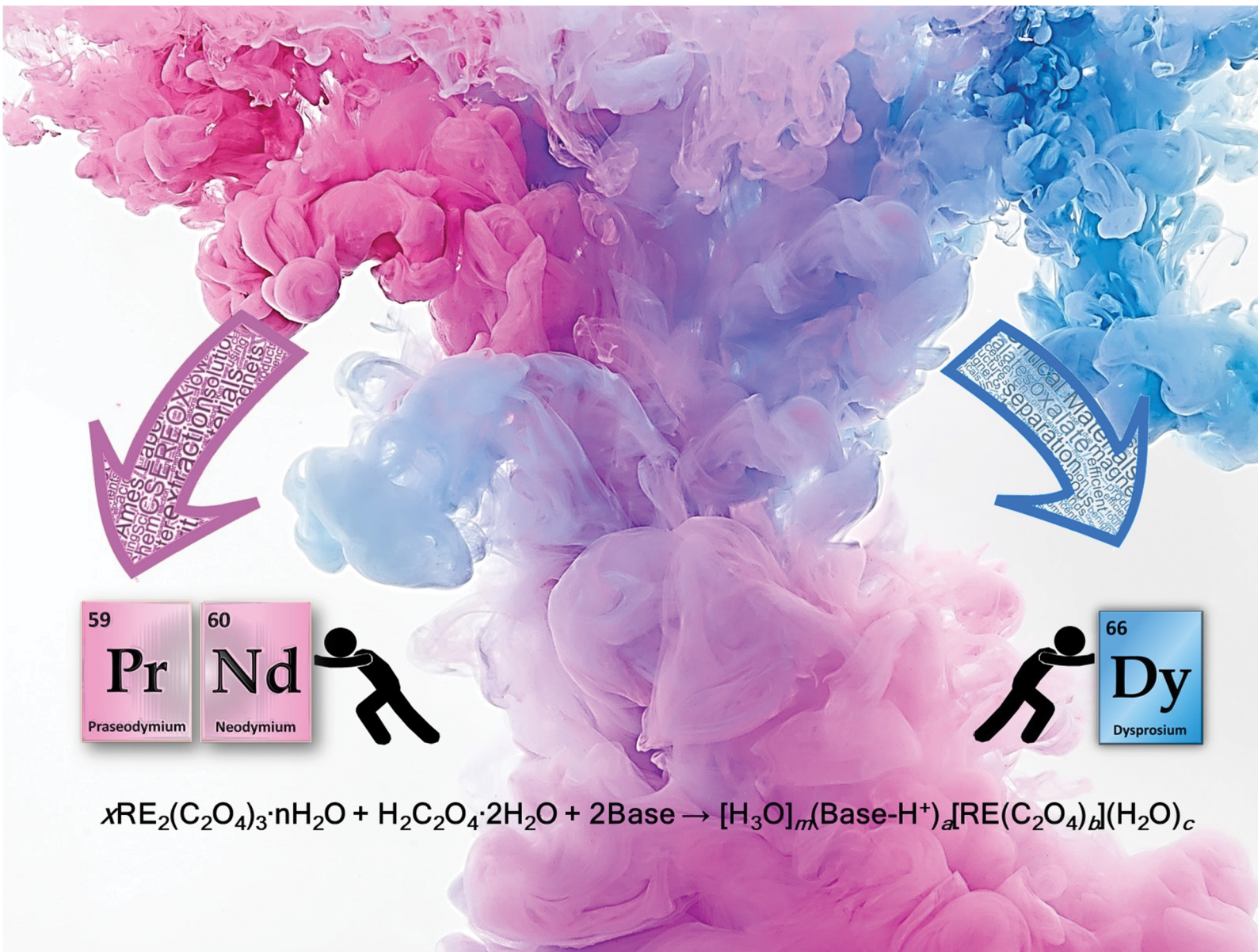


# ChemComm

Chemical Communications

rsc.li/chemcomm



ISSN 1359-7345



Cite this: *Chem. Commun.*, 2020, **56**, 11386

Received 28th March 2020,  
Accepted 7th May 2020

DOI: 10.1039/d0cc02270e

[rsc.li/chemcomm](http://rsc.li/chemcomm)

**A simple, environmentally benign, and efficient chemical separation of rare earth oxalates (CSEREOX) within two rare earth element (REE) subgroups has been developed. The protocol allows for selective solubilization of water-insoluble oxalates of rare earth elements, and results in efficient REE extraction even at low initial concentrations (<5%) from processed magnet wastes.**

The distinctive chemical and physical properties of rare earth elements (REEs) drive their growing demands in health care, electronics, transportation, aerospace, and defense applications. Low-carbon transition energy technologies including electric vehicles, and wind power depend strongly on neodymium and dysprosium for powerful magnets. The U.S. Department of Energy and the European Commission have categorized REEs as critical materials, due to their importance in the clean energy economy and the possibility of disruption in their supplies.<sup>1</sup> Forthcoming large scale implementation of the above-mentioned technologies will increase the demands for neodymium and dysprosium.<sup>2,3</sup> It is predicted that the demand for dysprosium and neodymium alone could rise by factors of 26 and 7, respectively, in the next 15 years.<sup>4</sup> The addition of costly dysprosium allows extending the use of Nd-Fe-B magnets to higher temperatures therefore some amounts of critical materials are needed to increase the performance of magnets. However, the natural source for dysprosium is the clays currently mined mainly in southern China

## Rationally designed rare earth separation by selective oxalate solubilization<sup>†</sup>

Denis Prodius, <sup>a</sup> Matthew Klocke, <sup>b</sup> Volodymyr Smetana, <sup>ac</sup> Tarek Alammar, <sup>b</sup> Marilu Perez Garcia, <sup>a</sup> Theresa L. Windus, <sup>ad</sup> Ikenna C. Nlebedim <sup>a</sup> and Anja-Verena Mudring <sup>abc</sup>

(Guangdong province).<sup>5</sup> Currently, the recycling rate is still very low (less than 1%).<sup>6,7</sup> A technological reason is the low concentration of these REEs in end-of-life products which makes extraction hard.<sup>8</sup> Also, the similarity in chemical properties of REEs makes separating them inherently problematic and represents a historic fundamental challenge in the field.<sup>9</sup> Solvent extraction is an important primary industrial technology for separation and purification of REEs but the process is complex and requires large scale usage of hazardous chemicals (e.g., organophosphorus compounds). Therefore, there is an economic, environmental, and strategic demand for developing novel efficient, low-cost extractants and extraction systems for separating rare earth metals as a group or from each other.

In this communication, we report on a straightforward, eco-friendly, and efficient chemical separation of REE in aqueous media within two subgroups: the lighter relatively low-priced elements, La-Sm (LRE), and the heavier, relatively high-priced elements, Gd-Lu (HRE). The processes for separating the heavy from light REEs (for example, <5% of Dy<sup>3+</sup> in Nd/Pr oxalate) are sufficiently selective (>68%) even at low concentrations.

The common method for recovery of REEs from permanent magnets is based on a hydrometallurgical approach.<sup>10</sup> The magnet alloys are dissolved in strong mineral acids (such as HCl, H<sub>2</sub>SO<sub>4</sub> or HNO<sub>3</sub>) and the REEs are recovered in the form of insoluble precipitate (oxalates, double sulphates or fluorides). The REE-containing sediment must be freed from non-REEs before it can be fed into an existing REE separation cycle. For recycling Nd-Fe-B magnet scrap, precipitated REE oxalates (REE = Nd, Pr, Dy) are thermally decomposed to obtain the corresponding REE oxides. Liquid-liquid extraction methods<sup>11</sup> are widely applied for separation of Nd/Pr and Dy but this process requires the presence of strong mineral acids. The process of fractional separation of rare earth by oxalate precipitation is also well-known,<sup>12-14</sup> but the efficiency of that process does not offer significant advantages over other methods like double sulphate or chromates salts precipitation.<sup>15</sup> The separation of rare earth oxalates in acidic<sup>12</sup> and basic<sup>13</sup> media is also established. The dissolution of several suitable RE

<sup>a</sup> Ames Laboratory, US Department of Energy and Critical Materials Institute, Ames, Iowa 50011-3020, USA

<sup>b</sup> Department of Materials Sciences and Engineering, Iowa State University, Ames, Iowa 50011-1096, USA

<sup>c</sup> Department of Materials and Environmental Chemistry, Stockholm University, Svante Arrhenius väg 16c, 10961 Stockholm, Sweden

E-mail: [anja-verena.mudring@mnmk.su.se](mailto:anja-verena.mudring@mnmk.su.se)

<sup>d</sup> Department of Chemistry, Iowa State University, Ames, Iowa 50011-3111, USA

<sup>†</sup> Electronic supplementary information (ESI) available: Detailed experimental procedures and characterization (IR, PXRD and Raman spectra, TG/DSC) of representative compounds, crystallographic information L1, L2-2H<sub>2</sub>O, 1-12 and computational studies. CCDC 1554317 (L1), 1554318 (L2-2H<sub>2</sub>O), 1554319-1554329 (1-12), unit cell data for 4. For ESI and crystallographic data in CIF or other electronic format see DOI: 10.1039/d0cc02270e



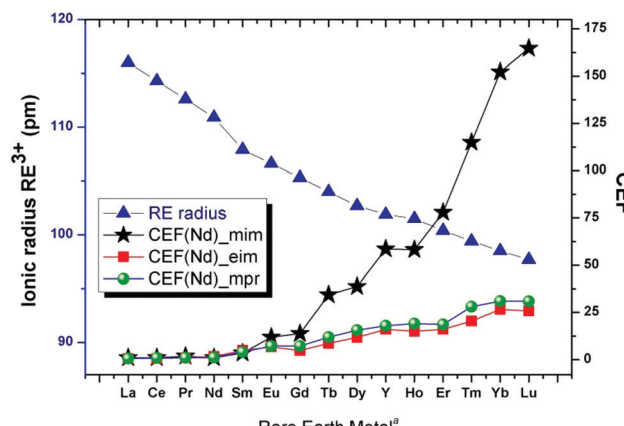


Fig. 1 Ionic radius and CEF as a function of different REE. Comparative extraction factors were based on the solubility of Nd(III) oxalate in water aided by 10 mmol of extractant. Spline curves are drawn to guide the eye. mim  $\equiv$  1-methylimidazole, eim  $\equiv$  1-ethylimidazole, mpr  $\equiv$  N-methylpyrrolidine.  
<sup>a</sup> Coordination number is equal to 8.

oxalates in 20% solutions of alkylamines oxalates (methyl, ethyl, triethyl) have been studied but with no great variation in the series of solubilities.<sup>16</sup> However, they still need essential improvements in light of optimizing critical parameters such as reaction time, separation medium (neutral pH), and overall fractionation efficiency for the mixed RE pairs with a non-equal element distribution (e.g., about 95% of Nd/Pr and 5% of Dy).

In our work the water-insoluble rare earth oxalates, which are the main intermediate products of the industrial production of REEs, are selectively reacted with an aqueous mixture of oxalic acid and an organic base (alkyl-imidazolium or alkyl-pyrrolidinium derivatives, see eqn (S1), ESI†) in a neutral pH.

This enables separation based on the solubility of the complex multifarious rare earth oxalates (Fig. 1). The light rare earth oxalates (LREOX) are practically insoluble compared to the heavy rare earth oxalates (HREOX) which allow for a selective transfer of the heavy rare earth to the liquid phase (Fig. 1). The ratio of solubility distributions (SDs)‡ between two independent components, defined as the concentrations of

dissolved rare earth oxalate ( $C_{RE}$ ) *versus* the least soluble one ( $C_{Nd}$ ), is stipulated here as the comparative extraction factor (CEF) using the corresponding base, CEF(Nd)\_base (eqn (1) and Fig. 1):

$$\text{CEF(Nd)}_{\text{base}} = C_{\text{RE}}/C_{\text{Nd}} \quad (1)$$

For a proof-of-concept, a Nd-Fe-B magnet obtained from the end-of-life electronic waste, was dissolved through an acid-free process<sup>17</sup> and subjected to the CSEREOX route.

Nd-Fe-B magnets typically contain Nd and Pr (a mixture of both elements is often called Didymium, represented as Di in Table 1). Dysprosium (Dy), which is considered even more critical, is added at lower a concentration for the higher temperature grades. Extraction of such low concentration of Dy from a mixture of REEs is a challenging problem, from both technical and economic perspective, even with standard separation methods. Applying the CSEREOX process to rare earth oxalates obtained from recycling the magnets from the motor in Fig. S1 (ESI†), enables reduction of the Dy content from 4.68 wt% to 1.49 wt% after extraction (proof-of-concept, line 8, Table 1). This illustrates the potential of the CSEREOX process for an efficient extraction (>68% extraction efficiency) of dysprosium(III) even at low concentrations as commonly encountered in end-of-life consumer products. A comparison of CSEREOX to other state-of-the-art recovery processes reveals important advantages (Table 1).

As efficient and industrially readily available bases, 1-methylimidazole (for separating Di and Dy) has been selected for a comparative analysis of the CSEREOX with state-of-the-art technologies. The CSEREOX approach proves to be operationally simple and faster. The use of commercially available and inexpensive starting materials and water as the only extraction medium, render the process economically attractive and potentially easy to deploy. 1-Methylimidazole, which allows for the best separation (Fig. 1), is one of the chemicals that has been classified by suppliers as a “Green Alternative Product”;<sup>22</sup> the use of REE oxalates *vs.* trifluoromethanesulfonate, chlorides or nitrates and water instead of organic solvents make the process

Table 1 Comparative analysis of REE separation processes

#	Parameter	Procedure		
		CSEREOX	TriNOx <sup>18</sup>	DEHPA <sup>19</sup>
1	Ligands	Commercial	3 steps, THF, $-78^{\circ}\text{C}$	Commercial
2	Phosphorous-ligands	No	No	Yes (+TBP)
3	RE source	Oxalates	RE(OTf) <sub>3</sub>	Chlorides, nitrates
4	Solvents	Only water	Et <sub>2</sub> O, <sup>a</sup> THF, <sup>a</sup> C <sub>6</sub> H <sub>6</sub> , <sup>b</sup> CHCl <sub>3</sub> <sup>b</sup>	#Kerosene, C <sub>6</sub> H <sub>14</sub> , H <sub>2</sub> O
5	Use of mineral acid	No	No	Yes
6	MSC	1	3	$\geq 3$
7	SF (Nd <i>vs.</i> Dy)	38 <sup>c</sup>	359	41.5
8	Proof-of-concept (Di <i>vs.</i> Dy)	4.68% <sup>d</sup>	25% <sup>e</sup>	Industrially applied (LLE)
9	Separation time	15 min	12 h	3 min <sup>20</sup> –55 h <sup>21</sup>

DEHPA (also known as D2EHPA) = di-(2-ethylhexyl)phosphoric acid; TBP = tributyl phosphate; OTf<sup>–</sup> = trifluoromethanesulfonate; <sup>a</sup> Flammable/explosive precursor; <sup>b</sup> Harmful or cancerogenic; MSC = minimum number of separation cycles; SF = separation factor; <sup>c</sup> Comparative extraction factor (CEF) for leaching with 1-methylimidazole as base; <sup>d</sup> Confirmed by XRF analysis as the dysprosium content in Nd-Fe-B magnets obtained from “Great Planes ElectriFly RimFire”, 10 35-30-1250 Outrunner Brushless Motor (Fig. S1, ESI); dysprosium content in didymium oxalate after extraction is 1.49% with extraction efficiency (EE) of (68.16%); <sup>e</sup> EE = 94.56%; liquid-liquid extraction method (LLE).

more benign. The new CSEREOX approach fulfills the principles of 'Green Chemistry'<sup>23</sup> with respect to atom economy, energy efficiency, less hazardous chemical synthesis using safer chemicals, solvents and/or auxiliaries.

To elucidate what leads to the solubilization and separation of the otherwise insoluble RE oxalates,<sup>24</sup> the structural motifs, coordination environment and effect of the base were examined using a combination of Raman spectroscopy and single crystal X-ray diffraction (SXRD). Crystal structures of REE-containing oxalate complexes obtained by the dissolution of RE oxalates in aqueous solution (**1–9**) as well as in ethanolic solution (**10–12**) and subsequent crystallization, have been determined, *i.e.*,  $[\text{mimH}][\text{Ho}(\text{ox})_2(\text{H}_2\text{O})]\cdot\text{H}_2\text{O}$  (**1**),  $[\text{mimH}][\text{Er}(\text{ox})_2(\text{H}_2\text{O})]\cdot1.5\text{H}_2\text{O}$  (**2**),  $[\text{mimH}][\text{RE}(\text{ox})_4]\cdot2\text{H}_2\text{O}$  (where RE  $\equiv$  Y (**3**), Yb (**4**), Lu (**5**));  $[\text{eimH}][\text{Ho}(\text{ox})_2(\text{H}_2\text{O})]\cdot\text{H}_2\text{O}$  (**6**),  $[\text{eimH}]_3[\text{Yb}(\text{ox})_3]\cdot2\text{H}_2\text{O}$  (**7**),  $[\text{mprH}]_8[\text{RE}_2(\text{ox})_7]\cdot10\text{H}_2\text{O}$  (where RE  $\equiv$  Tm (**8**), Yb (**9**)),  $[\text{H}_3\text{O}][\text{mimH}]_4[\text{RE}(\text{ox})_4]\cdot\text{H}_2\text{O}$  (RE  $\equiv$  Ho (**10**), Tm (**11**), Lu (**12**), see also Table S1 and Fig. S3–S5 (ESI<sup>†</sup>), for additional details. Structure analysis reveals that most commonly, the RE ion is coordinated exclusively by four oxalate ligands yielding isolated  $[\text{RE}(\text{ox})_4]^{5-}$  anion (*cf.* structures of **3**, **5**, **10–12**). With the *N*-methylpyrrolidinium cation, dimeric units formed by four oxalate ligands coordinated to each RE ion and one oxalate anion, bridging two RE ions, as found in **8** and **9**. With 1-ethylimidazole (eim) as the base the formation of a 1D zigzag chain of dimers, where two of the four oxalato ligands of a RE(III)-oxalate unit are shared between neighboring REE cations, is observed (**7**). Two similar types of 3D networks are found for compounds **6** (Ho, eim), **1** (Ho, mim), and **2** (Er, mim) (Fig. 2). In these structures, the common  $[\text{RE}(\text{ox})_4]^{5-}$  motif is observed. However, due to the larger size of Ho and Er

compared to Lu and Y, a water molecule enlarges the RE(III) coordination sphere from eight to nine. Each oxalate ligand is shared between two metals. The influence of the water activity on the coordination sphere is noteworthy and becomes evident when comparing the reaction products obtained from water and ethanol: in ethanolic solution, the formation of  $[\text{RE}(\text{ox})_4]^{5-}$  with an exclusive coordination of the RE(III) by oxalate ligands is preferred whilst in aqueous solution additional water can enter the coordination sphere of the RE(III) cation (compare (**10**) and (**1**)). The degree of condensation of the  $[\text{RE}(\text{ox})_4]^{5-}$  units is critically influenced by the base. With methylimidazolium cations, monomeric units are observed whereas methylpyrrolidinium gives rise to dimers for the same RE(III) (**4**) and (**11**) *vs.* (**8**) and (**9**)). Of the four crystal structures, for the larger Ho (**1**) and Er (**2**) compounds a nine-fold coordination of the RE(III) is observed, while for the relatively smaller Y (**3**) and Lu (**5**) eightfold coordination is observed. Although, the structures that form appear to be quite sensitive to the solvent used (water *vs.* 96% ethanol), the base employed during the reaction, the RE(III), all identified compounds show the RE(III) coordinated by four oxalate ligands. To confirm that the RE(III)-oxalate structure motifs evidenced by SXRD in solids are representative for the coordination of RE(III) in solution, comparative vibrational spectroscopy has been employed.

Raman spectra of representatives for the LRE and HRE subgroups in the solid (crystalline) form and in aqueous solution have been recorded and interpreted (ESI<sup>†</sup> Fig. S6 and S7). The solid-state vibrational spectra show, aside from stretching ( $3250$ – $2790\text{ cm}^{-1}$ ) and bending ( $1480$ – $510\text{ cm}^{-1}$ ) vibrations from the cation, modes that originate from C–O and RE–O bending and stretching modes associated with the complex anion. The  $[\text{mimH}]^+$ ,  $[\text{eimH}]^+$  and  $[\text{mprH}]^+$  Raman modes are very similar to those reported for other compounds containing these cations.<sup>25</sup> In solution, despite an increased noise-to-signal ratio due to the low concentration of some complexes (LRE) and weak Raman scattering, the RE–O (oxygen from the oxalate group) stretching and bending modes (for example,  $258\text{ cm}^{-1}$  and  $363\text{ cm}^{-1}$  in **3**) can still be identified (ESI<sup>†</sup> Fig. S6).<sup>25</sup> These findings indirectly confirm that the ions keep some of their structural integrity even in solutions. With this information, we conclude that the superior separation capabilities of methylimidazole compared to the other tested bases, lies in its ability to support the formation of isolated  $[\text{RE}(\text{ox})_4]^{5-}$  units for the heavier REE which have a higher solubility than any polymeric forms. This would provide an explanation for the synergistic play of REE ionic radius and base (*cf.* Fig. 1).

To provide a more thorough understanding of the comparative separation factors in REEs, the relative lanthanide oxalate binding energies were computed using density functional theory (DFT). For this, the ion exchange reaction, as described by eqn (2), was studied.  $\text{La}^{3+}$  and  $\text{Lu}^{3+}$  were chosen as representatives of the LREs and HREs, respectively.

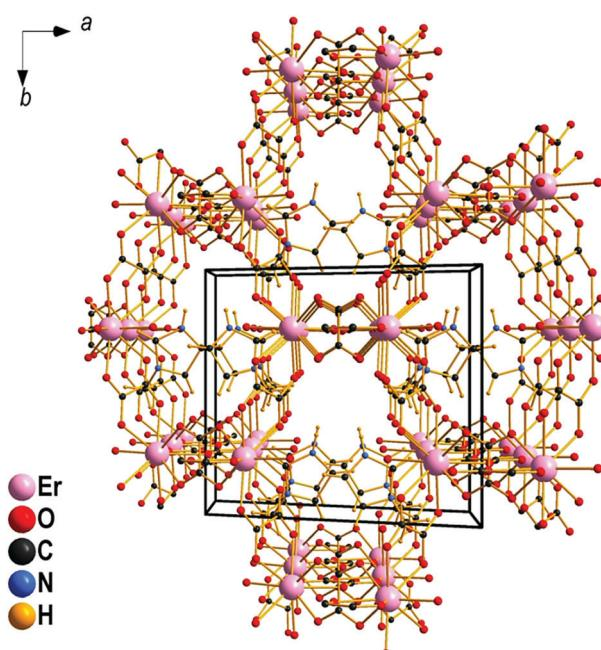
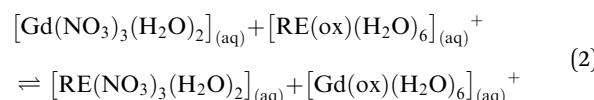


Fig. 2 The three-dimensional anionic network of  $[\text{Er}(\text{ox})_2]^-$  in **2** filled with  $[\text{mimH}]^+$  cations in hexagonal channels. Water molecules are omitted for clarity.



Nitrate, which is known to be a weakly coordinating ion in water,<sup>26</sup> was chosen to balance the charge on the RE ion. The calculated energies (Table S3, ESI†) show  $[\text{Lu}(\text{ox})(\text{H}_2\text{O})_6]^{+}$  has the largest relative binding energy;  $\sim 2 \text{ kcal mol}^{-1}$  more than for  $[\text{Gd}(\text{ox})(\text{H}_2\text{O})_6]^{+}$ . The La(III) and Gd(III) complexes have approximately equal binding energies with  $[\text{La}(\text{ox})(\text{H}_2\text{O})_6]^{+}$  being greater by only 0.02 kcal mol<sup>-1</sup>. This is in agreement with the experimental observation. Experimentally, it was found that the HRE-oxalates are more soluble according to eqn (1) and eqn (S1) (ESI†). From this, it would be expected that oxalate binds tighter to the HREs than the LREs. In addition, the experimentally determined RE-O bond lengths (2.31–2.41 Å) are comparable to the computational lengths from (2.13–2.68 Å) (Table S2, ESI†) providing assurance to the computational method accuracy. Thus, the strengths of the RE(III) oxalate binding which goes parallel with decreasing RE(III) ionic radius determines the complex formation, hence, selective dissolution which allows for effective REE separation.

In conclusion, a selective dissolution and separation of RE oxalates into an aqueous phase using environmentally benign chemicals such as oxalic acid was demonstrated. The CSEREOX procedure is simpler, faster, cheaper and far more environmentally benign than the currently used separation technologies. Its efficiency has been demonstrated by the successful extraction of dysprosium (EE > 68%) from the low dysprosium-containing material, as it is found in the recycling of original magnet (Nd–Fe–B) wastes. The REE separation relies on a synergistic interplay of the ionic radius (which goes hand in hand with the oxalate-RE binding strength) and the base, supporting the formation of isolated, soluble compounds.

AVM acknowledges financial support from the NSF (CHE-1465071) for the materials development and synthesis. Crystallographic, materials characterization and computational studies were supported by the Critical Materials Institute, an Energy Innovation Hub funded by the U.S. Department of Energy, Office of Energy Efficiency and Renewable Energy, Advanced Manufacturing Office (AVM, ICN, TLW). AVM acknowledges support from Stockholms Universitet and the Swedish Royal Academy of Science through the Göran Gustafsson awards that allowed completing the work.

## Conflicts of interest

There are no conflicts to declare.

## Notes and references

‡ Solubility distribution (SD) is defined here as the concentration of a rare earth oxalate in the aqueous extract phase.

1 (a) U.S. Department of Energy, *Critical Materials Strategy*, ed. D. Sandalow, Washington DC, 2011, pp. 1–191; (b) European Commission communication, Brussels, 13.9.2017, COM (2017) 490 final:

<https://ec.europa.eu/transparency/regdoc/rep/1/2017/EN/COM-2017-490-F1-EN-MAIN-PART-1.PDF>, accessed March 2020; (c) N. T. Nassar, J. Brainard, A. Gulley, R. Manley, G. Matos, G. Lederer, L. R. Bird, D. Pineault, E. Alonso, J. Gambogi and S. M. Fortier, *Sci. Adv.*, 2020, **6**, eaay8647.

- 2 A. Rollat, D. Guyonnet, M. Planchon and J. Tuduri, *Waste Manag.*, 2016, **49**, 427–436.
- 3 R. T. Nguyen, T. Fishman, F. Zhao, D. D. Imholte and T. E. Graedel, *Sci. Total Environ.*, 2018, **630**, 1143–1148.
- 4 E. Alonso, A. M. Sherman, T. J. Wallington, M. P. Everson, F. R. Field, R. Roth and R. E. Kirchain, *Environ. Sci. Technol.*, 2012, **46**, 3406–3414.
- 5 D. Powell, *Sci. News*, 2011, **180**, 18–21.
- 6 (a) S. M. Jowitt, T. T. Werner, Z. Weng and G. M. Mudd, *Curr. Opin. Green Sustain. Chem.*, 2018, **13**, 1–7; (b) M. Sethurajan, E. D. van Hullebusch, D. Fontana, A. Akcil, H. Deveci, B. Batinic, J. P. Leal, T. A. Gasche, M. A. Kucuker, K. Kuchta, I. F. F. Neto, H. M. V. M. Soares and A. Chmielarz, *Crit. Rev. Environ. Sci. Technol.*, 2019, **49**(3), 212–275.
- 7 K. Binnemans, P. T. Jones, B. Blanpain, T. Van Gerven, Y. Yang, A. Walton and M. Buchert, *J. Clean. Prod.*, 2013, **51**, 1–22.
- 8 A. Golev, M. Scott, P. D. Erskine, S. H. Ali and G. R. Ballantyne, *Resour. Policy*, 2014, **41**, 52–59.
- 9 (a) C. James, *J. Am. Chem. Soc.*, 1912, **34**(6), 757–771; (b) F. H. Spedding, A. F. Voigt, E. M. Gladrow and N. R. Sleight, *J. Am. Chem. Soc.*, 1947, **69**, 2777–2781; (c) X. Yin, Y. Wang, X. Bai, Y. Wang, L. Chen, C. Xiao, J. Diwu, S. Du, Z. Chai, T. E. Albrecht-Schmitt and S. Wang, *Nat. Commun.*, 2017, **8**, 14438–14446; (d) T. Cheisson and E. J. Schelter, *Science*, 2019, **363**, 489–493; (e) D. Kolodyska, D. Fila, B. Gajda, J. Gega and Z. Hubicki, in *Applications of Ion Exchange Materials in the Environment: Rare Earth Elements – Separation Methods Yesterday and Today*, ed. A. M. Inamuddin and A. Asiri, Springer, Switzerland, 2019, pp. 161–185.
- 10 H.-S. Yoon, C.-J. Kim, K.-W. Chung, S.-D. Kim, J.-Y. Lee and J. R. Kumar, *Hydrometallurgy*, 2016, **165**, 27–43.
- 11 F. Xie, A. A. Zhang, D. Dreisinger and F. Doyle, *Min. Eng.*, 2014, **56**, 10–28.
- 12 B. Weaver, *Anal. Chem.*, 1954, **26**, 479–480 and references therein.
- 13 L. A. Sarver and H. M.-P. Brinton, *J. Am. Chem. Soc.*, 1927, **49**, 943–958.
- 14 C. James, *J. Am. Chem. Soc.*, 1907, **29**, 495–499.
- 15 C. K. Gupta and N. Krishnamurthy, *Int. Mater. Rev.*, 1992, **37**, 197–248.
- 16 A. J. Grant and C. James, *J. Am. Chem. Soc.*, 1917, **39**, 933–937.
- 17 D. Prodius, K. Gandha, A.-V. Mudring and I. C. Nlebedim, *ACS Sustain. Chem. Eng.*, 2020, **8**(3), 1455–1463.
- 18 (a) J. A. Bogart, C. A. Lippincott, P. J. Carroll and E. J. Schelter, *Angew. Chem., Int. Ed.*, 2015, **54**, 8222–8225; (b) J. A. Bogart, B. E. Cole, M. A. Boreen, C. A. Lippincott, B. C. Manor, P. J. Carroll and E. J. Schelter, *Proc. Natl. Acad. Sci. U. S. A.*, 2016, **113**, 14887–14892.
- 19 F. Xie, T. A. Zhang, D. Dreisinger and F. Doyle, *Miner. Eng.*, 2014, **56**, 10–28.
- 20 M. Gergoric, C. Ekberg, B.-M. Steenari and T. Retegan, *J. Sustain. Metall.*, 2017, **3**(3), 601–610.
- 21 R. Bhave, D. Kim and E. S. Peterson, WO 2016/195831 Al, 2016.
- 22 Greener alternative products, <https://www.sigmaaldrich.com/chemistry/greener-alternatives/greener-alternative-products.html> accessed March 2020.
- 23 P. T. Anastas and J. C. Warner, *Green Chemistry: Theory and Practice*, Oxford University Press, New York, 1998, p. 135.
- 24 (a) C. E. Crouthamel and D. S. Martin Jr., *J. Am. Chem. Soc.*, 1950, **72**, 1382–1386; (b) C. E. Crouthamel and D. S. Martin Jr., *J. Am. Chem. Soc.*, 1951, **72**, 569–573.
- 25 V. H. Paschoal, L. F. O. Faria and M. C. C. Ribeiro, *Chem. Rev.*, 2017, **117**, 7053–7112.
- 26 R. M. Smith and A. E. Martell, *Critical Stability Constants*, Plenum, New York, NY, 1976, vol. 4, pp. 257.

